Monthly Notices
of the
ROYAL ASTRONOMICAL SOCIETY

MNRAS **494,** 2289–2298 (2020)
Advance Access publication 2020 March 29

doi:10.1093/mnras/staa850

Energy optimization in binary star systems: explanation for equal mass members in close orbits

Fred C. Adams,[1,2]★ Konstantin Batygin[3] and Anthony M. Bloch[4]

[1]*Physics Department, University of Michigan, Ann Arbor, MI 48109, USA*
[2]*Astronomy Department, University of Michigan, Ann Arbor, MI 48109, USA*
[3]*Division of Geological and Planetary Sciences, California Institute of Technology, Pasadena, CA 91125, USA*
[4]*Math Department, University of Michigan, Ann Arbor, MI 48109, USA*

Accepted 2020 March 19. Received 2020 February 9; in original form 2019 November 25

ABSTRACT

Observations indicate that members of close stellar binaries often have mass ratios close to unity, while longer period systems exhibit a more uniform mass-ratio distribution. This paper provides a theoretical explanation for this finding by determining the tidal equilibrium states for binary star systems – subject to the constraints of conservation of angular momentum and constant total mass. This work generalizes previous treatments by including the mass fraction as a variable in the optimization problem. The results show that the lowest energy state accessible to the system corresponds to equal mass stars on a circular orbit, where the stellar spin angular velocities are both synchronized and aligned with the orbit. These features are roughly consistent with observed properties of close binary systems. We also find the conditions required for this minimum energy state to exist: (1) the total angular momentum must exceed a critical value, (2) the orbital angular momentum must be three times greater than the total spin angular momentum, and (3) the semimajor axis is bounded from above. The last condition implies that sufficiently wide binaries are not optimized with equal mass stars, where the limiting binary separation occurs near $a_0 \approx 16 R_*$.

Key words: binaries: close – binaries: spectroscopic – stars: formation.

1 INTRODUCTION

A substantial fraction of the stellar population resides in binary systems, which can influence stellar properties and their long-term evolution. Binaries with short periods are especially important in this context, as they can experience mass transfer and affect the properties of both core-collapse and type Ia supernovae (De Marco & Izzard 2017). These processes, in turn, determine the merger rates for compact objects, including those that produce sources for gravitational waves (e.g. Narayan, Piran & Shemi 1991; Phinney 1991; Riles 2013; see also Lombardi et al. 2011). In order to understand these dynamical systems, previous studies have found the lowest energy states accessible to binaries, subject to conservation of angular momentum (Counselman 1973; Hut 1980). These optimized states correspond to circular orbits, where the angular velocities of both stars are synchronized with the orbit, with all three angular momentum vectors pointing in the same direction. These properties are often observed in close binary systems (e.g. Meibom, Mathieu & Stassun 2006; Mazeh 2008; see Shu 1982 for a textbook discussion). In addition, however, close binaries tend to have mass ratios that are closer to unity than the population as a whole (see below) and the origins of this trend remain elusive (note that previous calculations were carried out for systems with fixed stellar masses). The goal of this present work is to extend previous energy optimization calculations to include the apportionment of mass between the stellar members. Introducing this additional degree of freedom, we find that the critical point of the system is realized when the stars have equal masses. The existence of this tidal equilibrium state requires a minimum value for the total angular momentum. Moreover, in order for the critical point to be a true minimum of the energy, rather than a saddle point, the orbital angular momentum must be at least three times larger than the spin angular momentum. In addition, when the self-gravity of the stars is included in the energy budget, binary systems with equal mass correspond to energy minima only for sufficiently close orbits.

Although the observational landscape is complicated, members of close binary systems show a tendency towards equal masses, i.e. their mass ratios $q \equiv m_1/m_2$ are significantly closer to unity than would be expected if the secondaries sampled the full mass distribution (e.g. Tokovinin 2000; Halbwachs et al. 2003). In other words, sufficiently close binaries tend to be twins (Pinsonneault & Stanek 2006; El-Badry et al. 2019; cf. Lucy 2006). For solar-type stars with short periods, the mass ratio distribution tends to rise toward higher values (Mazeh et al. 1992; Duquennoy & Mayor

★ E-mail: fca@umich.edu

1991). A more recent survey (Moe & Di Stefano 2017) finds that about 30 per cent of close binaries (with $P < 20$ d and solar-type primaries) have mass ratios in the range $0.9 \leq q \leq 1$. Similarly, Raghavan et al. (2010) find that the distribution of mass ratios for short-period binaries with solar-type primaries has a well-defined peak near $q \sim 1$ (see also Duchene & Kraus 2013; Simon & Obbie 2009). An excess of twins (equal mass stars) is also observed for young binaries (Kounkel et al. 2019). For early-type stars, about 40 per cent of the close binary sample (with peak separation near $a \sim 0.15$ au) shows nearly equal masses $m_1 \approx m_2$ (Kobulnicky & Fryer 2007; cf. Kobulnicky, Kiminki & Lundquist 2014). A similar result holds for a separate study where the primaries are A-type stars (De Rosa et al. 2014). The data thus show a significant excess of nearly equal mass stars for close binaries. Moreover, the aforementioned studies indicate that the distribution of mass ratios is significantly different for wider binaries. Undoubtedly, the interplay of physical processes that leads to the distributions of mass ratios for different binary separations is complex, and can only be understood through detailed calculations. Instead of taking this route, this paper provides a partial explanation for these observational trends by showing that the lowest energy state accessible to close binary systems has equal mass stars.

The general problem of finding the lowest energy states of a physical system, subject to constraints, has a long history in astrophysics (dating back to Darwin 1879, 1880). Previous applications include binary star systems with fixed angular momentum (Counselman 1973; Hut 1980), and ellipsoidal figures of equilibrium for both isolated stars and binaries (Chandrasekhar 1969; Lai, Rasio & Shapiro 1993; Levine et al. 1993); these latter studies focus on energy optimization with respect to the compressibility and oblateness of the stars, whereas this paper focuses on optimization of the mass ratios. Tidal equilibrium states[1] have also been found for planetary systems containing Hot Jupiters (Levrard, Winisdoerffer & Chabrier 2009; Adams & Bloch 2015), and for hierarchical triple systems (Adams & Bloch 2016). This procedure has been generalized for applications to multiplanet systems with fixed orbital spacing (Adams 2019), where the optimal state corresponds to planets with nearly equal masses. However, this prediction of mass uniformity breaks down when self-gravity of the planets is included and the total mass of the system is sufficiently large (Adams et al. 2020). Although calculations of this type – by design – gloss over the machinery of the dissipative effects at play, they provide a powerful means of illuminating the general outlines of dynamical evolution, subject to energy damping.

This paper is organized as follows. We formulate the optimization problem in Section 2. In this treatment, the system energy is a function of 10 dimensionless variables, subject to conservation of angular momentum (which provides three constraints). Section 3 derives the tidal equilibrium state, which corresponds to equal mass stars on a circular orbit, with the orbital angular momentum and stellar angular momentum aligned. In Section 4, we consider the second variation and find the conditions required for the critical point to be the minimum of the energy. Section 5 then compares the predictions of this calculation with current observational data. The paper concludes in Section 6 with a summary of our results and a discussion of their implications.

[1]Note that the term 'tidal equilibrium state' refers to the configuration of lowest energy, which can be reached through any type of energy dissipation – not necessarily tidal forcing.

2 FORMULATION OF THE OPTIMIZATION PROBLEM

For binary systems, the energy budget includes the orbital energy, the stellar spins, and the self-gravity of the constituent stars. The total system energy can thus be written in the form

$$\mathcal{E} = -\frac{Gm_1m_2}{2a_0} - \alpha_g\frac{Gm_1^2}{R_1} - \alpha_g\frac{Gm_2^2}{R_2} + \frac{1}{2}I_1\Omega_1^2 + \frac{1}{2}I_2\Omega_2^2. \quad (1)$$

Here, the stars have masses m_k, radii R_k, and moments of inertia I_k, where the Ω_k are the magnitudes of the stellar angular velocity vectors. The semimajor axis of the orbit is given by a_0 and α_g is a dimensionless factor of order unity (the constant α_g depends on the internal structure and is assumed to be the same for both stars; see Appendix A for further discussion).

The square of the magnitude of the orbital angular momentum is given by

$$h^2 = G\frac{m_1^2m_2^2}{m_1+m_2}a_0(1-e^2), \quad (2)$$

where e is the eccentricity of the binary orbit. The total angular momentum can be written in the form

$$\boldsymbol{\mathcal{L}} = \boldsymbol{h} + I_1\boldsymbol{\Omega}_1 + I_2\boldsymbol{\Omega}_2. \quad (3)$$

For the sake of definiteness, we define the coordinate system so that the total angular momentum vector $\boldsymbol{\mathcal{L}}$ points in the $\hat{z}$-direction and the orbital angular momentum vector $\boldsymbol{h}$ lies in the x–z plane. The angular velocity vectors of the stars can in principle have components in all three directions.

The individual stellar masses are allowed to vary, but their sum M_T is assumed to be constant, so that

$$m_1 + m_2 = M_T = \text{constant}. \quad (4)$$

We define the mass fraction f so that

$$f = \frac{m_1}{M_T} \qquad \text{and} \qquad 1-f = \frac{m_2}{M_T}. \quad (5)$$

For the stars, we adopt the approximate mass–radius relation

$$R_k = R\left(\frac{m_k}{M_T}\right)^{1/2}, \quad (6)$$

where R is a constant (e.g. see Prialnik 2000). The scale R is the radius of a star with mass M_T at the time when the masses of the two stars are being determined. As a result, both stars have radii $R_k < R$. Moreover, since the masses are determined during the early phases of evolution, R is expected to be larger than the main-sequence value. With this choice of mass–radius relation, we can write the moments of inertia in the form

$$I_k = \eta\, m_k R_k^2 = \eta\, M_T R^2\left(\frac{m_k}{M_T}\right)^2, \quad (7)$$

where η is a dimensionless quantity of order unity and is assumed to be the same for both stars. Note that both α_g and η are determined by the density distributions of the stars.

Next we define dimensionless quantities,

$$a = \frac{a_0}{R}, \qquad E = \frac{\mathcal{E}R}{GM_T^2}, \qquad L = \frac{\mathcal{L}}{M_T(GM_TR)^{1/2}},$$
$$\omega_k^2 = \frac{\Omega_k^2R^3}{GM_T}. \quad (8)$$

The expression for the dimensionless energy then takes the form

$$E = -\frac{1}{2a} f(1-f) - \alpha_{\rm g}[f^{3/2} + (1-f)^{3/2}] + \frac{1}{2}\eta\left[\omega_1^2 f^2 + \omega_2^2 (1-f)^2\right], \quad (9)$$

where the dimensionless angular velocities each have three components so that

$$\omega_1^2 = \omega_{1x}^2 + \omega_{1y}^2 + \omega_{1z}^2 \qquad \text{and} \qquad \omega_2^2 = \omega_{2x}^2 + \omega_{2y}^2 + \omega_{2z}^2. \quad (10)$$

The components of the dimensionless angular momentum become

$$L_z = L = \sqrt{a} f(1-f)\cos i\sqrt{1-e^2} + \eta f^2 \omega_{1z} + \eta(1-f)^2\omega_{2z}, \quad (11)$$

$$L_x = 0 = \sqrt{a} f(1-f)\sin i\sqrt{1-e^2} + \eta f^2 \omega_{1x} + \eta(1-f)^2\omega_{2x}, \quad (12)$$

and finally

$$L_y = 0 = \eta f^2 \omega_{1y} + \eta(1-f)^2\omega_{2y}. \quad (13)$$

The energy scale used in equation (8) is comparable to the binding energy of the stars, and $a \gtrsim 1$, so the dimensionless energy E is generally less than unity. The angular momentum scale is comparable to that of a contact binary with total mass M_T, so that the dimensionless angular momentum L is generally greater than unity. The dimensionless stellar rotation rates ω_k are scaled to the break-up speeds for a star of mass and radius (M_T, R). As a result, the stellar spins $\omega_k < 1$, the spin angular momenta $S_k \sim \eta\omega_k < 1$, so that most of the angular momentum typically resides in the orbit.

3 EQUILIBRIUM STATES: THE FIRST VARIATION

We need to find the minimum energy state for the system defined through equation (9), subject to the constraint of constant angular momentum (given by equations 11–13). The energy and angular momentum depend on the 10 variables, i.e.

$$E = E(\boldsymbol{X}), \qquad \boldsymbol{L} = \boldsymbol{L}(\boldsymbol{X}),$$
$$\boldsymbol{X} = (a, e, i, \omega_{1x}, \omega_{1y}, \omega_{1z}, \omega_{2x}, \omega_{2y}, \omega_{2z}, f). \quad (14)$$

For each variable (denoted here as ξ), the optimization condition has the form

$$\frac{\partial E}{\partial \xi} + \boldsymbol{\lambda}\cdot\frac{\partial \boldsymbol{L}}{\partial \xi} = 0, \quad (15)$$

where the vector $\boldsymbol{\lambda} \equiv (\lambda_x, \lambda_y, \lambda_z)$ is the Lagrange multiplier.

For semimajor axis a, we obtain the condition

$$\frac{1}{2a^2} f(1-f) + \frac{1}{2} a^{-1/2} f(1-f)\sqrt{1-e^2}\,[\lambda_z \cos i + \lambda_x \sin i] = 0. \quad (16)$$

Note that solutions exist for the cases where $f = 0$ or 1, whereas we are interested in $f \neq 0$, 1.

Next we consider the eccentricity, which results in the condition

$$-\frac{e}{\sqrt{1-e^2}}\sqrt{a} f(1-f)\,[\lambda_z \cos i + \lambda_x \sin i] = 0, \quad (17)$$

and the inclination angle, which requires

$$\sqrt{a} f(1-f)\sqrt{1-e^2}\,[-\lambda_z \sin i + \lambda_x \cos i] = 0. \quad (18)$$

For components of the stellar rotation rate of the first star, all three equations have the form

$$\eta f^2\,[\omega_{1a} + \lambda_a] = 0, \quad (19)$$

where the index a runs over the three components ($a = x, y, z$). Similarly, for the stellar rotation rate of the second star we find

$$\eta(1-f)^2\,[\omega_{2a} + \lambda_a] = 0. \quad (20)$$

Finally, we consider the mass fraction f, which leads to the more complicated expression

$$-\frac{1}{2a}(1-2f) - \alpha_{\rm g}\frac{3}{2}\left[f^{1/2} - (1-f)^{1/2}\right] + \eta\left[\omega_1^2 f - \omega_2^2(1-f)\right] + \sqrt{a(1-e^2)}\,[\lambda_z \cos i + \lambda_x \sin i](1-2f) + 2\eta f\boldsymbol{\lambda}\cdot\boldsymbol{\omega}_1 - 2\eta(1-f)\boldsymbol{\lambda}\cdot\boldsymbol{\omega}_2 = 0. \quad (21)$$

The solution to the first variation equations (16)–(21), in conjunction with the definitions of the angular momentum components (11)–(13), yield the solution for the equilibrium point. The orbit must be circular and aligned with the stellar spins so that

$$\boxed{e = i = \omega_{1x} = \omega_{2x} = \omega_{1y} = \omega_{2y} = 0.} \quad (22)$$

In addition, the stellar spin periods must match the orbital period, and the stars have equal mass, so that the non-zero system parameters have values

$$\boxed{\omega_{1z} = \omega_{2z} = a^{-3/2} \qquad \text{and} \qquad f = 1/2.} \quad (23)$$

The existence of the critical point implies a consistency constraint. The angular momentum must be sufficiently large in order for the critical point to exist. This result follows from evaluating the angular momentum from equation (11) using the values (22) and (23) at the critical point, which leads to the expression

$$L = \frac{1}{4}\left[\omega^{-1/3} + 2\eta\omega\right], \quad (24)$$

where we have suppressed the subscript on the stellar angular velocity ω. This expression has a minimum value where

$$\omega = \left(\frac{1}{6\eta}\right)^{3/4}, \quad (25)$$

which implies the constraint

$$\boxed{L > L_{\rm min} = \frac{1}{3}\,[6\eta]^{1/4}.} \quad (26)$$

If this condition is not met, then no critical point exists. In this case, the binary system can attain a lower energy state by shrinking the orbit – and spinning up the stars to conserve angular momentum. Note that the minimum L constraint is evaluated at the critical point where $f = 1/2$, corresponding to equal mass stars. In this case, the minimum angular momentum corresponds to an extremely close orbit (some type of contact binary) so that equation (26) is almost always satisfied. In contrast, this minimum angular momentum does provide non-trivial constraints for binary systems with extreme mass ratios (see Levrard et al. 2009; Adams & Bloch 2015).

Fig. 1 shows a contour plot of the energy as a function of the mass fraction f and the semimajor axis a of the binary orbit. In order to illustrate basic trends, the eccentricity, inclination angle, and stellar spin components are specified to be those of the tidal equilibrium state (given by equations 22 and 23). The stellar structure parameters are taken to be $\eta = 0.2$ and $\alpha_{\rm g} = 0.15$. In this state, the angular momentum $L = \sqrt{a}/4 + \eta/(2a^{3/2})$, so the values of a in the diagram

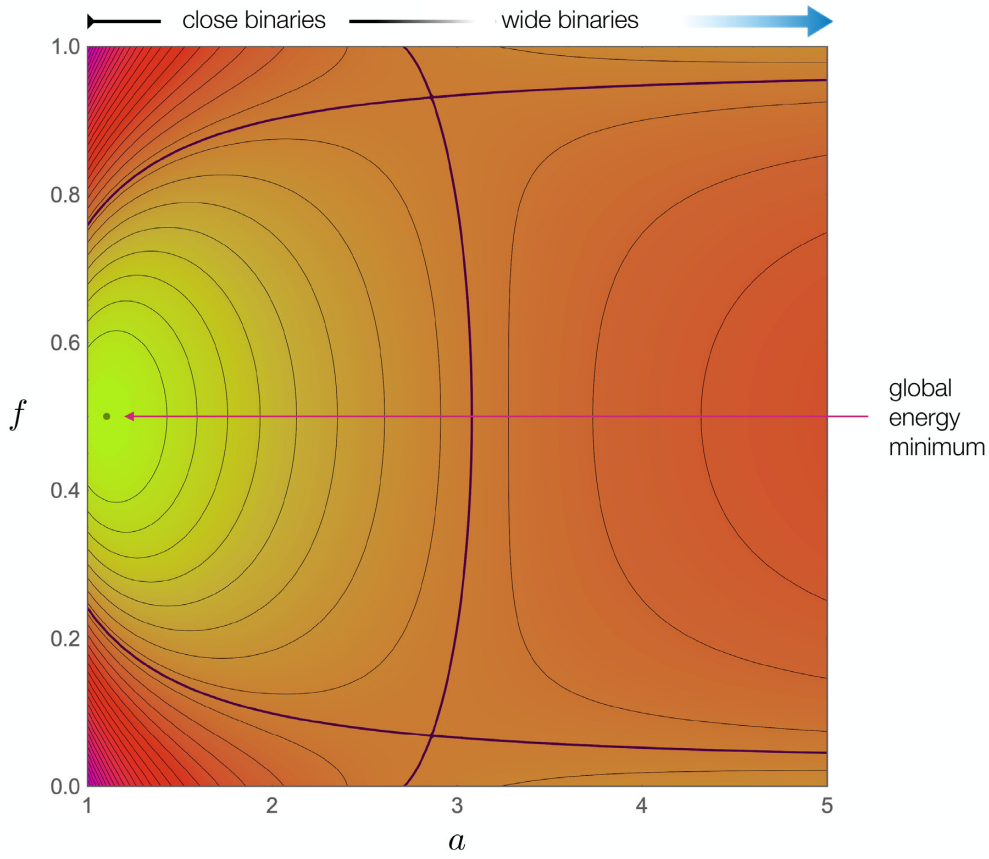

Figure 1. Contour plot showing the energy as a function of the mass fraction f and the semimajor axis a of the binary orbit (in dimensionless form). The other variables are taken to be those of the tidal equilibrium state, so that $e = i = \omega_{1x} = \omega_{2x} = \omega_{1y} = \omega_{2y} = 0$, and $\omega_{1z} = \omega_{2z} = a^{-3/2}$. The region shaded yellow (centred on $f = 1/2$ for small a) represents the lowest energy states available to the system over this part of the plane, and corresponds to equal mass stars. At larger values of a, however, the energy has a maximum at $f = 1/2$ (shaded orange on the right-hand side of the diagram). In this region, lower energy states are available as $f \to 0$, 1, favouring stars with unequal masses. The transition from an energy minimum to an energy maximum occurs at $a \approx 3$ (for this choice of parameters – see the text).

correspond to different choices of total angular momentum. For small semimajor axis, $a \sim$ 1–2, Fig. 1 displays a well-defined minimum for nearly equal mass stars with $f = 1/2$ (shown as the yellow region). This energy minimum for $f = 1/2$ turns into a maximum for larger semimajor axes (shown as the orange region on the right-hand side of the diagram), with the transition near $a \gtrsim 3$. However, the strength of the maximum at large a (as measured by the energy difference between $f = 1/2$ and 0, 1) is much weaker than the depth of the energy minimum at small a. This asymmetry implies that the tendency for close binaries to have equal masses should be stronger than the tendency for wider binaries (here $a \gtrsim 3$) to have small mass ratios.

Although Fig. 1 illustrates basic trends, many of the independent variables have been suppressed. The following section considers the full second variation of the energy function and thus provides a more robust assessment of the conditions required for the tidal equilibrium state to be a minimum energy state.

4 STABILITY OF THE CRITICAL STATE: THE SECOND VARIATION

In order to show that the critical point found in the previous section corresponds to a stable equilibrium point, we must consider the second variation. For this analysis, it is useful to explicitly conserve angular momentum (instead of using Lagrange multipliers), so that we write the expression for the energy in the form

$$E = -\frac{1}{2a} f(1-f) - \alpha_g \left[f^{3/2} + (1-f)^{3/2} \right] + \frac{1}{2}\eta (1-f)^2 \times \left[\omega_{2x}^2 + \omega_{2y}^2 + \omega_{2z}^2 \right] + \frac{1}{2\eta f^2} \left[S_{1x}^2 + S_{1y}^2 + S_{1z}^2 \right]. \quad (27)$$

For shorthand notation, we have defined the components of the spin angular momentum of the first star as

$$S_{1z} \equiv \left[L - \sqrt{a} f(1-f) \cos i \sqrt{1-e^2} - \eta (1-f)^2 \omega_{2z} \right],$$

$$S_{1x} \equiv -\left[\sqrt{a} f(1-f) \sin i \sqrt{1-e^2} + \eta (1-f)^2 \omega_{2x} \right],$$

$$\text{and} \qquad S_{1y} \equiv -\eta (1-f)^2 \omega_{2y}. \quad (28)$$

This formulation of the problem explicitly enforces conservation of angular momentum.

We now take derivative with respect to all of the remaining variables. For the binary semimajor axis a:

$$E_a = \frac{1}{2a^2} f(1-f) - \frac{1}{2\eta f^2} \left[a^{-1/2} f(1-f) \sqrt{1-e^2} \right] \times \left[S_{1x} \sin i + S_{1z} \cos i \right]. \quad (29)$$

For the eccentricity e:

$$E_e = \frac{1}{\eta f^2}\left[S_{1x}\sin i + S_{1z}\cos i\right]\left[\sqrt{a}f(1-f)\right]\frac{e}{\sqrt{1-e^2}}. \quad (30)$$

For the inclination angle i:

$$E_i = \frac{1}{\eta f^2}[S_{1x}\cos i - S_{1z}\sin i][-\sqrt{a}f(1-f)\sqrt{1-e^2}] \quad (31)$$

For the components of the stellar angular velocity ω_{2k}, we get three expressions:

$$E_{\omega 2z} = \eta(1-f)^2\omega_{2z} - \frac{1}{f^2}\left[S_{1z}(1-f)^2\right], \quad (32)$$

$$E_{\omega 2x} = \eta(1-f)^2\omega_{2x} - \frac{1}{f^2}\left[S_{1x}(1-f)^2\right], \quad (33)$$

and

$$E_{\omega 2y} = \eta(1-f)^2\omega_{2y} - \frac{1}{f^2}\left[S_{1y}(1-f)^2\right]. \quad (34)$$

And finally for the mass fraction f:

$$\begin{aligned} E_f = &-\frac{1}{2a}(1-2f) - \alpha_g\frac{3}{2}[f^{1/2} - (1-f)^{1/2}] \\ &- \eta(1-f)\omega_2^2 - \frac{1}{\eta f^3}\left[S_{1x}^2 + S_{1y}^2 + S_{1z}^2\right] \\ &+ \frac{1}{\eta f^2}\{S_{1x}[-\sqrt{a}(1-2f)\sin i\sqrt{1-e^2} + \eta 2(1-f)\omega_{2x}]\} \\ &+ \frac{1}{\eta f^2}\{S_{1y}\eta 2(1-f)\omega_{2y} \\ &+ S_{1z}[-\sqrt{a}(1-2f)\cos i\sqrt{1-e^2} + \eta 2(1-f)\omega_{2z}]\}. \end{aligned} \quad (35)$$

Next we find (again) the critical point. The solution corresponds to $e = i = 0$, $\omega_{1x} = \omega_{2x} = 0$, $\omega_{1y} = \omega_{2y} = 0$, and $\omega_{1z} = \omega_{2z} = \omega \neq 0$. With these specifications, the remaining two equations can be evaluated.

For the $E_a = 0$ condition, we obtain

$$\frac{1}{a^{3/2}}\eta f^2 = S_{1z} = L - h - \eta\omega(1-f)^2. \quad (36)$$

For the $E_f = 0$ condition, we obtain

$$\begin{aligned} E_f = &-\frac{1}{2a}(1-2f) - \alpha_g\frac{3}{2}\left[f^{1/2} - (1-f)^{1/2}\right] \\ &- \eta(1-f)\omega^2 - \frac{1}{\eta f^3}\left[S_{1z}^2\right] \\ &+ \frac{1}{\eta f^2}\left\{S_{1z}\left[-\sqrt{a}(1-2f) + \eta 2(1-f)\omega\right]\right\} = 0. \end{aligned} \quad (37)$$

The first condition shows that $\omega = a^{-3/2}$ so that $S_{1z} = \eta\omega f^2$. Using these results, the final equation has solution $f = 1/2$. We thus recover the same critical point found earlier, as expected (see equations 22, 23).

Next we need to evaluate the Hessian matrix and find its eigenvalues, or at least find the criteria necessary for the eigenvalues to be positive (Hesse 1872). First consider the second derivatives with respect to a single variable. For the semimajor axis matrix element, we find the expression

$$E_{aa} = \frac{1}{16a^3}\left[-3 + \frac{a^2}{\eta}\right]. \quad (38)$$

For the eccentricity matrix element, we get

$$E_{ee} = \frac{1}{4}\omega\sqrt{a} = \frac{1}{4a}. \quad (39)$$

For the inclination matrix element, we get

$$E_{ii} = \frac{1}{4}\omega\sqrt{a} + \frac{a}{4\eta} = \frac{1}{4a} + \frac{a}{4\eta}. \quad (40)$$

The second derivatives with respect to each of the components ω_{2a} all have the same form,

$$E_{\omega 2x,\omega 2x} = E_{\omega 2y,\omega 2y} = E_{\omega 2z,\omega 2z} = \frac{\eta}{2}. \quad (41)$$

The second f derivative has the form

$$\begin{aligned} E_{ff} = &\frac{1}{a} - \alpha_g\frac{3}{4}\left[f^{-1/2} + (1-f)^{-1/2}\right] + \eta\omega^2 \\ &+ (1/\eta f^2)\left[-\sqrt{a}(1-2f) + \eta 2(1-f)\omega\right]^2 \\ &+ (S_{1z}/\eta f^2)\left[2\sqrt{a} - 2\eta\omega\right] - (4S_{1z}/\eta f^3) \\ &\times \left[-\sqrt{a}(1-2f) + \eta 2(1-f)\omega\right] + 3S_{1z}^2/(\eta f^4). \end{aligned} \quad (42)$$

This expression can be evaluated at the critical point and simplified to find the matrix element

$$E_{ff} = \frac{3}{a} - \alpha_g\frac{3}{2}\sqrt{2} - \frac{2\eta}{a^3}. \quad (43)$$

Now we consider the mixed derivatives. For derivatives involving the semimajor axis, $E_{a\xi}$, the only non-zero term is

$$E_{a\omega 2z} = \frac{1}{8\sqrt{a}}. \quad (44)$$

For the case of eccentricity, $E_{e\xi} = 0$ for all mixed derivatives. For inclination angle, $E_{i\xi}$, the only non-zero term is

$$E_{i\omega 2x} = \frac{\sqrt{a}}{4}. \quad (45)$$

All of the other terms are zero.

Here, we order the variables according to $(a, \omega_{2z}, i, \omega_{2x}, e, \omega_{2y}, f)$. The entire 7×7 Hessian matrix $\mathbb{H}$ takes the block diagonal form

$$\mathbb{H} = \begin{bmatrix} \mathbb{A} & 0 & 0 \\ 0 & \mathbb{B} & 0 \\ 0 & 0 & \mathbb{C} \end{bmatrix}, \quad (46)$$

where the submatrices are defined as follows: for the variables (a, ω_{2z}), we obtain the 2×2 matrix

$$\mathbb{A} = \begin{bmatrix} (a^2 - 3\eta)/(16\eta a^3) & 1/8\sqrt{a} \\ 1/8\sqrt{a} & \eta/2 \end{bmatrix}. \quad (47)$$

For the variables (i, ω_{2x}), we find a second 2×2 matrix that takes the form

$$\mathbb{B} = \begin{bmatrix} 1/4a + a/4\eta & \sqrt{a}/4 \\ \sqrt{a}/4 & \eta/2 \end{bmatrix}. \quad (48)$$

For the remaining three variables (e, ω_{2y}, f), all of the mixed derivatives vanish, so that we obtain the diagonal 3×3 matrix

$$\mathbb{C} = \begin{bmatrix} 1/4a & 0 & 0 \\ 0 & \eta/2 & 0 \\ 0 & 0 & 3/a - \alpha_g 3\sqrt{2}/2 - 2\eta/a^3 \end{bmatrix}. \quad (49)$$

The eigenvalues of the 2×2 submatrix $\mathbb{A}$ for the variables (a, ω_{2z}) are determined by the solution to the quadratic equation

$$\begin{aligned} &\lambda^2 - [(a^2 - 3\eta)/(16\eta a^3) + \eta/2]\lambda + (a^2 - 3\eta)/(32a^3) \\ &\quad - 1/64a = 0, \end{aligned} \quad (50)$$

which has solutions

$$2\lambda = \left[\frac{a^2-3\eta}{16\eta a^3}+\frac{\eta}{2}\right] \pm \left\{\left[\frac{a^2-3\eta}{16\eta a^3}+\frac{\eta}{2}\right]^2 - \left[\frac{a^2-3\eta}{8a^3}-\frac{1}{16a}\right]\right\}^{1/2}. \quad (51)$$

Both eigenvalues will be positive provided that the final term in square brackets is positive, which enforces the condition

$$a^2 > 6\eta. \quad (52)$$

Since we do not need the eigenvalues themselves – only their signs – this constraint can also be derived by showing that the matrix is positive definite (so that it has only positive eigenvalues). From Sylvester's Criterion, a real-symmetric matrix is positive definite if and only if all its leading principal minors are positive (Gilbert 1991). Applying this criterion to the matrix $\mathbb{A}$ leads to the result (52).

The interpretation of the constraint (52) is that the system can only enter into its equilibrium state if the orbital angular momentum h is sufficiently large compared to the total spin angular momentum $S_T = I_1\omega_1 + I_2\omega_2$. In dimensionless units, in the critical state, $h = \sqrt{a}/4$ and $S_T = (1/2)\eta a^{-3/2}$, so the ratio $h/S_T = a^2/2\eta$. Equation (52) thus implies that the orbital angular momentum must be at least three times greater than the total spin angular momentum in order for the extremal state to be an energy minimum (and hence stable), i.e.

$$\boxed{h > 3S_T = 3(S_1 + S_2).} \quad (53)$$

The eigenvalues of the 2×2 submatrix $\mathbb{B}$ for the variables (i, ω_{2x}) are given by the quadratic

$$\lambda^2 - \left(\frac{1}{4a}+\frac{a}{4\eta}+\frac{\eta}{2}\right)\lambda + \frac{\eta}{2}\left(\frac{1}{4a}+\frac{a}{4\eta}\right) - \frac{a}{16} = 0, \quad (54)$$

which has solutions

$$2\lambda = \left(\frac{1}{4a}+\frac{a}{4\eta}+\frac{\eta}{2}\right) \pm \left\{\left(\frac{1}{4a}+\frac{a}{4\eta}+\frac{\eta}{2}\right)^2 - \left(\frac{\eta}{2a}+\frac{a}{4}\right)\right\}^{1/2}. \quad (55)$$

Both of these eigenvalues are always positive.

The eigenvalues of the third 3×3 matrix $\mathbb{A}$ for the variables (e, ω_{2y}, f) are given by the diagonal elements. The first two are manifestly positive. The final eigenvalue for the mass fraction f has the form

$$\lambda_f = \frac{3}{a} - \alpha_g\frac{3\sqrt{2}}{2} - \frac{2\eta}{a^3}. \quad (56)$$

Stability requires that $\lambda_f > 0$, which is turn places a constraint on the system parameters

$$\alpha_g < \frac{\sqrt{2}}{a}\left[1 - \frac{2\eta}{3a^2}\right]. \quad (57)$$

Alternately, the maximum binary separation for which there is a stable equilibrium configuration is given by

$$a < a_{\max} \approx \frac{\sqrt{2}}{\alpha_g}. \quad (58)$$

Note that for a polytropic star, the self-gravity parameter α_g is given by

$$\alpha_g(n) = \frac{3}{2(5-n)}, \quad (59)$$

where n is the polytropic index. For low-mass stars, $n = 3/2$, $\alpha_g = 3/7$, and $a_{\max} = 7\sqrt{2}/3 \sim 3.3$. The semimajor axis is written in units of the stellar radius parameter R. For the equilibrium state, each stellar radius has the value $R_k = R(m_k/M_T)^{1/2} = R/\sqrt{2}$, so that the system has a minimum separation $a_{\min} \sim \sqrt{2}/2 \approx 0.71$ (note that contact binaries actually allow for somewhat closer orbits). In addition, however, the semimajor axis must satisfy the constraint of equation (52) in order for the equilibrium state to be a minimum. This condition implies that $a \geq (6\eta)^{1/2}$. For pre-main-sequence stars, the dimensionless moment of inertia $\eta \approx 1/5$, so that $a \geq (6/5)^{1/2} \approx 1.10$. As a result, the full range of allowed binary orbits for which it is energetically favourable to have equal mass is given by

$$1.1 \lesssim a \lesssim \frac{\sqrt{2}}{\alpha_g} \sim 3.3. \quad (60)$$

The dimensionless semimajor axis a is given in terms of the length scale R, so that the stellar radii $R_k = R/\sqrt{2}$ for equal mass stars. Newly formed stars and young pre-main-sequence stars are larger than their main-sequence counterparts by factors of 3–4 (for solar-type stars, e.g. Stahler & Palla 2005). Taking these results into account, the upper bound on the semimajor axis in physical units becomes

$$a_0 \lesssim 16R_{*(\mathrm{MS})}, \quad (61)$$

where $R_{*(\mathrm{MS})}$ is the main-sequence radius of the star. One should also keep in mind that binary separations can evolve after the epoch of formation. As a result, some binaries with nearly equal masses can form in tight orbits, within the limit of equation (61), but then increase their semimajor axes afterwards. In addition, the specific values presented here depend on the stellar mass–radius relation from equation (6). However, the exact form of the mass–radius relation depends on the mass range of the stars and the stage of evolution when the stellar masses are determined, so that the limit of equation (61) should be considered approximate (see Appendix A for further discussion of how variations in the stellar structure parameters affect the optimization procedure).

For completeness, we note that when binaries are close enough to favour equal mass members, they are also close enough to strongly interact through magnetic fields during their pre-main-sequence phase. More specifically, the magnetic truncation radius (e.g. Shu et al. 1994) for circumstellar discs is comparable to the separation of equation (60). In addition, this orbital separation $a \sim 10R_*$ is roughly the maximum semimajor axis for which binary stars are affected by tidal interactions over their main-sequence lifetimes (e.g. Hurley, Tout & Pols 2002).

5 COMPARISON WITH OBSERVATIONS

The analysis of this paper indicates that equal mass stars are energetically favoured, but the critical point is a true minimum only for close binaries that satisfy the constraint of equation (61). As outlined in Introduction, observations suggest that the population of close binaries displays a modest excess of nearly equal mass stars, but the distribution of mass ratios spans the full range of possible values. None the less, sufficiently close binaries should favour equal mass members. The goal of this section is to search for such a signature in the currently available data.

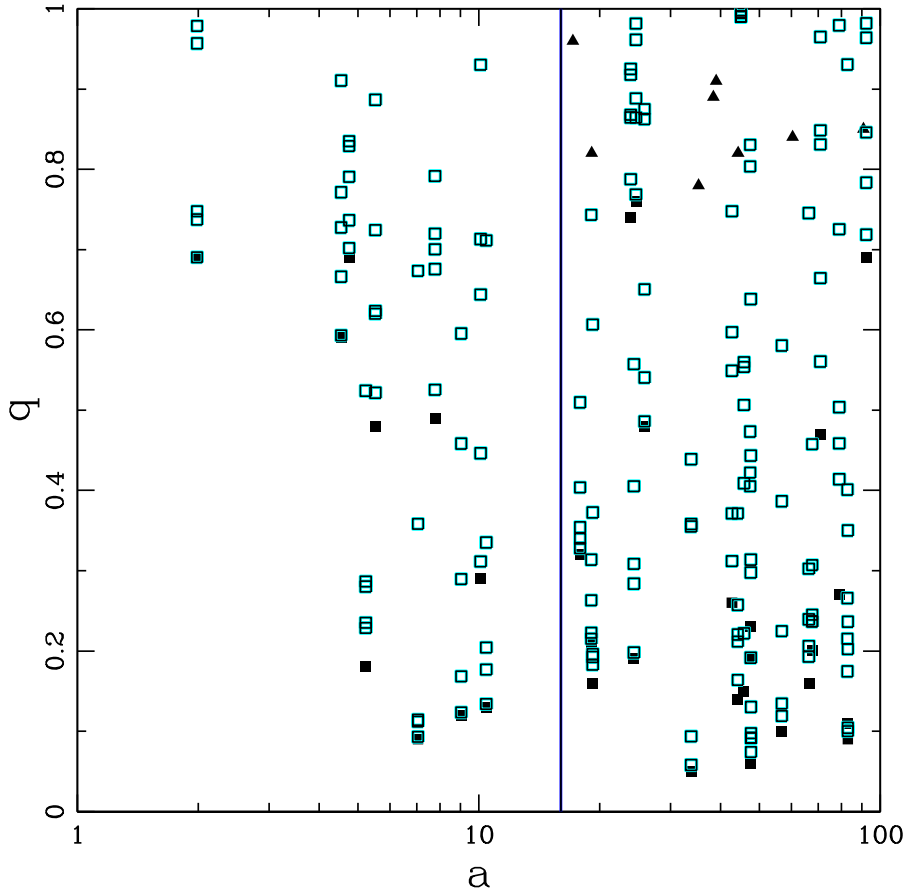

Figure 2. Mass ratios q for a collection of spectroscopic binaries (from Mazeh et al. 2003) as a function of separation (in units of the primary radius). Solid black squares depict the minimum values of the mass ratio q for single-lined spectroscopic binaries. The open cyan squares show realizations of the mass ratios obtained by sampling the possible inclination angles. The solid black triangles depict the mass ratios obtained for the double-lined spectroscopic binaries in the sample. The vertical blue line delineates the boundary between close binary systems for which equal mass stars are favoured (left) and wider binary systems (right).

As one example, we consider the sample of spectroscopic binaries compiled by Mazeh et al. (2003). The paper reports the mass ratios for 52 single-lined (table 1) and 11 double-lined spectroscopic binaries (table 2) with primary masses in the range $m_1 = 0.6$–$0.85\,M_\odot$. For the single-lined category, observations measure the composite quantity f_M given by

$$f_M = \frac{(m_2 \sin i)^3}{(m_1 + m_2)^2} = \frac{(q \sin i)^3}{(1+q)^2}, \tag{62}$$

where m_1 (m_2) is the mass of the primary (secondary), i is the inclination angle, and q is the mass ratio. The mass of the primary can be independently estimated, so that the observations determine the minimum value of the mass ratio, q_{min}, defined as the value of q that corresponds to an edge-on orbit ($i = \pi/2$). In contrast, for double-lined spectroscopic binaries, the additional data available allow for an estimate of the inclination angle and hence q itself (see also Shahaf, Mazeh & Faigler 2017 for a detailed discussion of the observational complexities).

The observational data from the aforementioned sample are presented in Fig. 2, which plots the estimated mass ratios versus the semimajor axes of the systems. Three types of data are presented: the solid squares show the minimum value of the mass ratio for the observed single-lined spectroscopic binaries. The open squares show realizations of the mass ratio obtained from sampling $\sin i$ (and inverting equation 62 to find q). The mass ratios for the double-lined spectroscopic binaries are shown as the solid triangles in the figure. The constraint from equation (61) is shown as the vertical blue line in the diagram. Although the data span a wide distribution, the points to the left of the line (for close binaries) tend to have somewhat larger mass ratios than those on the right (wider binaries), roughly consistent with theoretical expectations.

For sufficiently close binaries, it is energetically favourable for the stars to have equal masses. For binaries wider than the limit (61), which comprise the majority of systems (e.g. Duchene & Kraus 2013), it is energetically favourable for one star to accrete most of the mass. However, the collection of mass ratios shown in Fig. 2 does not show a sharp transition between close binaries with equal masses and wider binaries with much smaller mass ratios. In general, observations of binary mass ratios show both a moderate preference for equal masses and an overall distribution that is relatively flat (see e.g. Duquennoy & Mayor 1991; Mazeh et al. 1992; Tokovinin 2000; Halbwachs et al. 2003). The preference for equal mass stars is often characterized in terms of an excess of systems with high mass ratios $0.95 < q < 1$, where the excess fraction is typically $\mathcal{F}_{\rm eq} \sim 0.1 - 0.2$ for close binaries and decreases significantly with orbital period (Raghavan et al. 2010; Moe & Di Stefano 2017). However, the distribution is not skewed heavily toward extreme values. The fact that this dominance does not usually occur places constraints on the star formation process. In particular, binary formation is complicated and energy dissipation is inefficient. Tidal interactions provide one important source of dissipation for binary systems, but they have a steep dependence on semimajor axis (Hut

1981) and become ineffective for binaries wider than the limit of equation (61).

For binaries that are wide enough so that the equal mass state ($f = 1/2$) is not a minimum, we can derive a lower limit on the mass fraction f (equivalently, the mass ratio $q = f/[1-f]$) by requiring that the tidal equilibrium state remains a minimum for arbitrary mass ratios. If we redo the analysis of the previous section, but consider the mass fraction to be an input parameter rather than a variable to be optimized over, the criterion (53) for the tidal equilibrium state to be a minimum takes the more general form

$$\sqrt{a}\, f(1-f) > 3\eta a^{-3/2} \left[f^2 + (1-f)^2 \right] . \tag{63}$$

This result implies that the orbital angular momentum must be greater than three times the spin angular momentum (as found previously; Hut 1980). This expression can be rewritten as a constraint on the mass fraction

$$\frac{1}{2} - \frac{1}{2} \left(\frac{1 - 6\eta/a^2}{1 + 6\eta/a^2} \right)^{1/2} < f < \frac{1}{2} + \frac{1}{2} \left(\frac{1 - 6\eta/a^2}{1 + 6\eta/a^2} \right)^{1/2} . \tag{64}$$

In the limit $\eta \ll a^2$, this constraint simplifies to the (leading order) form

$$\frac{3\eta}{a^2} < f < 1 - \frac{3\eta}{a^2} . \tag{65}$$

The tidal equilibrium state is no longer a minimum of the energy for mass fractions outside this range (equivalently, for mass ratios $q < 3\eta/a^2$). However, this constraint is rather weak: if we ignore factors of order unity (e.g. 3η) the limit on the companion mass takes the form $m_2 \gtrsim M_T (R_*/a_0)^2$. For solar-type stars, e.g. the limit on m_2 falls below the minimum stellar mass for $a_0 \gtrsim 0.1$ au.

6 CONCLUSION

This paper has found the tidal equilibrium states for binary star systems, including the optimization of the masses of the constituent members. In this formulation of the problem, the spins of both stars and the binary orbit contribute to the angular momentum, which is held constant. This work generalizes previous treatments by allowing mass to be apportioned between the two stars, subject to conservation of total mass, and by including the self-gravity of the stars in the energy budget.

6.1 Summary of results

The properties of the tidal equilibrium state (equations 22, 23) are analogous to those found earlier without considering mass as a variable (Hut 1980). The stellar spins are synchronous and aligned with the binary orbit, which has zero eccentricity. The existence of the minimum energy state requires the system to have a minimum total angular momentum (equation 26). In addition, in order for the equilibrium state to be an energy minimum, the orbital angular momentum must at least three times larger than the spin angular momentum (equation 53).

The main result of this analysis is that the tidal equilibrium state for binary systems corresponds to equal mass stars. If we include the self-gravity of the stars in the energy budget, then in order for the tidal equilibrium state to be a minimum, the semimajor axis of the binary must be bounded from above (equations 58, 61). As a result, equal mass stars are only energetically advantageous in sufficiently close binary systems (equation 60). The maximum semimajor axis for binaries that favour equal mass stars occurs for separations $a_0 \sim 16 R_{*(\mathrm{MS})}$ (where $R_{*(\mathrm{MS})}$ is the main-sequence radius of the star). These properties are roughly consistent with the observed population of binary systems, where close binaries have a preference for equal mass members and wider binaries display a different (more diverse) distribution of mass ratios.

The treatment of this paper assumes that the mass–radius relation (6) holds for both stellar members of the binary. It also assumes that both stars have the same structure, i.e. the constants α_g and η that depend on the internal mass distribution of the stars are the same for both objects. The finding that equal mass stars provides the lowest energy state is largely independent of the particular functional form of the mass–radius relation, but does depend on the equality of the structure constants (see Appendix A). However, the form of the mass–radius relation does affect the range of binary separations over which the equilibrium state is an energy minimum. Since the internal structure of forming and newly formed (pre-main-sequence) stars evolves with time, the assumption of a common mass–radius relation requires the stars to form at approximately the same time.

6.2 Discussion

This analysis indicates that energy considerations favour equal mass stars for sufficiently close binaries, in agreement with observations (although the picture is complex, as discussed in Sections 1 and 5). However, most binaries are too wide for this result to apply, so that the tidal equilibrium state (with the mass ratio as a variable) becomes a saddle point over most of the parameter space. Only sufficiently close binaries are affected by the energy optimization procedure carried out in this paper (equation 61).

The results presented here are based on global energy considerations, and are independent of the possible pathways by which the binary systems realize such states. None the less, some mechanism(s) for energy loss must be in operation, and the dissipation time-scale must be short compared to the time-scale for star formation, i.e. $t_{\mathrm{diss}} \ll t_{\mathrm{form}}$. Although equal mass stars are favoured for close binaries, not all systems will achieve their optimal state. As a result, close binaries are expected to display a range of mass ratios, but still show a tendency for mass ratios closer to unity. For wider binaries, it is not energetically favourable to have equal masses. Moreover, the stars in such systems are generally too far apart to interact, either by mass transfer during the formative stages or by tidal interactions afterwards, so that the stars can be considered largely independent.

The constraints of this paper are robust, in that the lowest energy states are independent of the evolutionary trajectory by which the binary systems are formed. In particular, the tidal equilibrium state does not depend on the mechanism(s) by which the system loses energy. At the same time, this treatment is necessarily incomplete. Any source of dissipation can lead to the systems evolving toward lower energy states, but we would none the less like to know the specific routes through which binary star systems determine their mass ratios and orbital properties (e.g. see Tohline 2002; Duchene & Kraus 2013; Moe & Kratter 2018, and references therein). This goal remains a formidable challenge for the future.

ACKNOWLEDGEMENTS

We would like to thank Kaitlin Kratter, Darryl Seligman, and Chris Spalding for useful discussions. We also thank the referee for useful input. This work was supported through the University of Michigan, the National Science Foundation, the Air Force Office of Scientific Research, the David and Lucile Packard Foundation, and the Alfred P. Sloan Foundation.

REFERENCES

Adams F. C., 2019, MNRAS, 488, 1446
Adams F. C., Batygin K., Bloch A. M., Laughlin G., 2020, MNRAS, 493, 5520
Adams F. C., Bloch A. M., 2015, MNRAS, 446, 3676
Adams F. C., Bloch A. M., 2016, MNRAS, 462, 2527
Chandrasekhar S., 1969, Ellipsoidal Figures of Equilibrium. Yale Univ. Press, New Haven. CT
Counselman C. C., 1973, ApJ, 180, 307
Darwin G. H., 1879, The Observatory, 3, 79
Darwin G. H., 1880, Phil. Trans. R. Soc. A, 171, 713
De Rosa R. J. et al., 2014, MNRAS, 437, 1216
De Marco O., Izzard R. G., 2017, PASA, 34, e001
Duchêne G., Kraus A., 2013, ARA&A, 51, 269
Duquennoy A., Mayor M., 1991, A&A, 248, 485
El-Badry K., Rix H.-W., Tian H., Duchêne G., Moe M., 2019, MNRAS, 489, 5822
Gilbert G. T., 1991, Am. Math. Mon., 98, 44
Halbwachs J. L., Mayor M., Udry S., Arenou F., 2003, A&A, 397, 159
Hesse L. O., 1872, Die Determinanten Elementar Behandelt. Leipzig
Hurley J. R., Tout C. A., Pols O. R., 2002, MNRAS, 329, 897
Hut P., 1980, A&A, 92, 167
Hut P., 1981, A&A, 99, 126
Kobulnicky H. A., Fryer C. L., 2007, ApJ, 670, 747
Kobulnicky H. A. et al., 2014, ApJS, 213, 34
Kounkel M. et al., 2019, AJ, 157, 196
Lai D., Rasio F. A., Shapiro S. L., 1993, ApJS, 88, 205
Levine A., Rappaport S., Deeter J. E., Boynton P. E., Nagase F., 1993, ApJ, 410, 328
Levrard B., Winisdoerffer C., Chabrier G., 2009, ApJ, 692, 9
Lombardi J. C., Holtzman W., Dooley K. L., Gearity K., Kalogera V., Rasio F. A., 2011, ApJ, 737, 49
Lucy L. B., 2006, A&A, 629, 635
Mazeh T., Simon M., Prato L., Markus B., Zucker S., 2003, ApJ, 599, 1344
Mazeh T., 2008, Tidal Effects in Stars, Planets, and Disks, in M. J. Goupil and J. P. Zahn (eds). EAS Publication Series, Vol. 29, p. 1
Mazeh T., Goldberg D., Duquennoy A., Mayor M., 1992, ApJ, 401, 265
Meibom S., Mathieu R. D., Stassun K. G., 2006, ApJ, 653, 621
Moe M., Di Stefano R., 2017, ApJS, 230, 15
Moe M., Kratter K. M., 2018, ApJ, 854, 44
Narayan R., Piran Z., Shemi A., 1991, ApJ, 379, 17
Phinney E. S., 1991, ApJ, 380, 17
Pinsonneault M. H., Stanek K. Z., 2006, ApJ, 639, L67
Prialnik A., 2000, An Introduction to the Theory of Stellar Structure and Evolution. Cambridge Univ. Press, Cambridge
Raghavan D. et al., 2010, ApJS, 190, 1
Riles K., 2013, Part. Nucl. Phys., 68, 1
Shahaf S., Mazeh T., Faigler S., 2017, MNRAS, 472, 4497
Shu F. H., 1982, The Physical Universe. University Science Books, Mill Valley, CA
Shu F., Najita J., Ostriker E., Wilkin F., Ruden S., Lizano S., 1994, ApJ, 429, 781
Simon M., Obbie R. C., 2009, AJ, 137, 3442
Stahler S. W., Palla F., 2005, The Formation of Stars. Wiley, New York,
Tohline J. E., 2002, ARA&A, 40, 349
Tokovinin A. A., 2000, A&A, 360, 997

APPENDIX A: GENERALIZED FORMS FOR THE STELLAR STRUCTURE PARAMETERS

In order to carry out the optimization calculation, we had to specify the mass–radius relationship (6) and the dimensionless structure constants (η and α_g) for the stars. In this appendix we assess how these choices affect the results. We can generalize the calculation further in two directions, by considering the mass–radius relationship to be an arbitrary function, and by considering the structure constants to have different values for the two stars.

For a generalized version of the mass–radius relation, the stellar radii R_k can be written in the form

$$R_1 = RH_{(f)} \qquad \text{and} \qquad R_2 = RH_{(1-f)}, \tag{A1}$$

where H is an arbitrary (dimensionless) function and R is the same radial scale used previously [so that $H(1) = 1$ and $R = R_*(M_T)$]. In equation (A1), the function H is evaluated at f for the first star and at $1 - f$ for the second star. We use a smaller font for the arguments to distinguish the evaluation of the function from the multiplication of the function by the argument. With this ansatz, the energy of self-gravity becomes

$$E_{\rm grav} = -\left[\alpha_1 \frac{f^2}{H_{(f)}} + \alpha_2 \frac{(1-f)^2}{H_{(1-f)}}\right] \equiv -\left[\alpha_1 \Gamma_{(f)} + \alpha_2 \Gamma_{(1-f)}\right], \tag{A2}$$

where the second equality defines a new dimensionless function Γ. Note that the α_k can be different for the two stars. Similarly, the moments of inertia have the generalized forms

$$I_1 = \eta_1 M_T R^2 H^2_{(f)} \qquad \text{and} \qquad I_2 = \eta_2 M_T R^2 H^2_{(1-f)}. \tag{A3}$$

The dimensionless energy and angular momentum terms for stellar spin take the modified forms

$$E_{\rm spin} = \frac{1}{2}\eta_1 \omega_1^2 H^2_{(f)} + \frac{1}{2}\eta_2 \omega_2^2 H^2_{(1-f)}, \tag{A4}$$

and

$$\boldsymbol{L}_{\rm spin} = \eta_1 H^2_{(f)} \boldsymbol{\omega}_1 + \eta_2 H^2_{(1-f)} \boldsymbol{\omega}_2. \tag{A5}$$

For taking the first variation (Section 3), only the derivatives with respect to the mass fraction f are affected by the generalization. These new terms have forms

$$\frac{\partial E_{\rm grav}}{\partial f} = \alpha_1 \Gamma'_{(f)} - \alpha_2 \Gamma'_{(1-f)}, \tag{A6}$$

$$\frac{\partial E_{\rm spin}}{\partial f} = \eta_1 \omega_1^2 H_{(f)} H'_{(f)} - \eta_2 \omega_2^2 H_{(1-f)} H'_{(1-f)}, \tag{A7}$$

and

$$\frac{\partial \boldsymbol{L}_{\rm spin}}{\partial f} = \eta_1 H_{(f)} H'_{(f)} \boldsymbol{\omega}_1 - \eta_2 H_{(1-f)} H'_{(1-f)} \boldsymbol{\omega}_2, \tag{A8}$$

where the primes represent derivatives of the functions Γ and H with respect to their argument. Given that the critical point corresponds to $\boldsymbol{\omega}_1 = \boldsymbol{\omega}_2 = \omega\hat{z}$, all of the above expressions vanish for the choice $f = 1 - f = 1/2$ when the structure constants are equal ($\alpha_1 = \alpha_2 = \alpha_g$ and $\eta_1 = \eta_2$). As a result, the critical point remains the same, even for an arbitrary mass–radius relation, i.e. the tidal equilibrium point corresponds to equal mass stars.

This result – equal mass stars – requires that the functions specifying the self-gravity and the moment of inertia are the same for both stars. If they are different functions, either with different constants (α_k, η_k) or different functional forms (Γ, H), then the tidal equilibrium point will not always correspond to equal mass stars. If the structure functions are 'almost' the same, then we expect the critical point to have almost equal mass stars. However, the departure from equality will depend on the functions in question, so that a more general result is beyond the scope of this paper.

Similarly, the Hessian matrix elements for the second variation (Section 4) depend on the form of the generalized mass–radius relation H and the ancillary function Γ. The range of parameter space for which the eigenvalues are positive, so that the

critical point is an energy minimum, will thus depend on the form of these functions. For example, if we change the power-law index of the mass–radius relation of equation (6), then the dimensionless function appearing in the generalized self-gravity contribution of equation (A2) will have a power-law form $\Gamma(x) = x^p$. The eigenvalue corresponding to the mass fraction has the form

$$\lambda_f = E_{ff} = \frac{3}{a} - \frac{2\eta}{a^3} - \alpha_{\rm g}\, p\,(p-1)\, 2^{3-p}, \tag{A9}$$

where we have assumed that $\alpha_1 = \alpha_2 = \alpha_{\rm g}$. Different values for the index p will thus change the range of semimajor axes for which the eigenvalue is positive and for which the tidal equilibrium state is an energy minimum.

This paper has been typeset from a TEX/LATEX file prepared by the author.